Wind and Structures, Vol. 8, No. 2 (2005) 89-106
DOI: http://dx.doi.org/10.12989/was.2005.8.2.089

Wind induced vibrations of long electrical overhead transmission line spans: a modified approach

Himanshu Verma† and Peter Hagedorn‡

Institut für Mechanik, Technische Universität Darmstadt, Hochschulstraβe-1, D-64289, Darmstadt, Germany

(Received January 1, 2004, Accepted July 1, 2004)

Abstract. For estimating the vortex excited vibrations of overhead transmission lines, the Energy Balance Principle (EBP) is well established for spans damped near the ends. Although it involves radical simplifications, the method is known to give useful estimates of the maximum vibration levels. For very long spans, there often is the need for a large number of in-span fittings, such as in-span Stockbridge dampers, aircraft warning spheres etc. This adds complexity to the problem and makes the energy balance principle in its original form unsuitable. In this paper, a modified version of EBP is described taking into account in-span damping and in particular also aircraft warning spheres. In the first step the complex transcendental eigenvalue problem is solved for the conductor with in-span fittings. With the thus determined complex eigenvalues and eigenfunctions a modified energy balance principle is then used for scaling the amplitudes of vibrations at each resonance frequency. Bending strains are then estimated at the critical points of the conductor. The approach has been used by the authors for studying the influence of in-span Stockbridge dampers and aircraft warning spheres; and for optimizing their positions in the span. The modeling of the aircraft warning sphere is also described in some detail.

Keywords: energy balance principle; overhead transmission lines; Stockbridge damper; warning sphere; transcendental eigenvalue problem.

1. Introduction

In this paper we are concerned exclusively with the vibrations in the frequency range of 3 to 50 Hz due to von Kármán vortex shedding in a wide range of wind speeds (1−7 m/sec) (EPRI 1979). Although such vibrations are barely perceptible due to their low amplitudes (less than a conductor diameter), they can however be extremely important since they may lead to material fatigue at points of high conductor curvature.

Dampers of the Stockbridge type or other designs are often placed near the suspension clamps to suppress these vibrations. The dynamic characteristics of the Stockbridge dampers are often described by its complex impedance, which is a function of frequency and of the amplitude of motion of the damper clamp. Particularly in long spans dampers are also mounted in groups (2 to 5 dampers in each group) not only near the ends of the span but also in-span. This is the case

† Corresponding Author, E-mail: himanshu@mechanik.tu-darmstadt.de
‡ E-mail: hagedorn@mechanik.tu-darmstadt.de

whenever geographical conditions (e.g. Fjord or river crossings etc.) force engineers to lay the transmission lines of fairly big span lengths, which may fall in the range of few thousand meters, and hence, are installed with a large number of Stockbridge dampers and aircraft warning spheres. The location of the dampers in the span as well as their dynamic characteristics are of importance and have to be modeled with sufficient detail. The problem was studied by means of the Ritz-Galerkin and the finite element method (Dhotarad, *et al*. 1978, Allnut and Rowbottom 1974), in which the conductor was modeled by the wave equation. The frequencies of interest (typically 3-50 Hz) lie in the range from the 500th to the 1000th eigenfrequency for a long span transmission line. A large number of shape functions (in the case of Ritz-Galerkin method) or the elements (in the case of finite element method) has therefore to be considered in these computations in order to obtain sufficiently good results.

In the case of a conductor with damping near the span-ends only, the problem is simplified in the usual EBP calculations. Since the eigenfrequencies for a typical transmission lines are closely spaced (in the order of 0.1 Hz), the discrete spectrum, being relatively dense, can be approximated by the continuous spectrum of an infinite or semi-infinite conductor (Schäfer 1981). Energy balance is then carried out for all the frequencies of the range of interest and very simple expressions can be obtained for an average free-field vibration amplitude for each wind speed (Hagedorn 1980, 1982, Hagedorn, *et al*. 2002). Also, approximate expressions are obtained for the bending strains and simple conditions for the optimal tuning of the damper and its location near the span end can be derived. The approach gives fairly good results. For long spans with in-span damping and aircraft warning spheres this simple approach is no longer feasible, since the relative positions of the fittings become important and the vibrations can no longer be represented by a single average free-field amplitude. The vibration levels may now differ considerably along the span and this is reflected in the vibration modes.

In the present paper, therefore the EBP is presented in a form in which first a transcendental eigenvalue problem is formulated for the conductor with in-span fittings, analogous to Hagedorn, *et al*. (2002), Verma, *et al*. (2003), and then applying EBP to the individual complex vibration modes. The numerical difficulties associated to the solution of the transcendental eigenvalue problem were overcome by normalizing the basic variables and by adopting appropriate method for solving the eigenvalue problem. The modeling of the aircraft warning spheres is also discussed and an realistic example is solved and discussed.

2. Modeling of a long span with in-span fittings

Fig. 1 shows a typical single conductor transmission line equipped with N conductor fittings (i.e. Stockbridge dampers and/or warning spheres). The span length L, i.e., the distance between the towers, can be of the order of few thousand meters, while the conductor's sag is of the order of just a few percent of the span length. On the other hand, the frequencies under consideration (i.e. 3-50 Hz) correspond to wave lengths of a few meters only, so that for the purpose of the present study the sag can be disregarded, the conductor being modeled as a taut string (with some bending stiffness). In a first approximation the conductor vibrations can be assumed to occur mainly in the vertical direction. The vibrations in the nth sub-span are then described by the partial differential equation

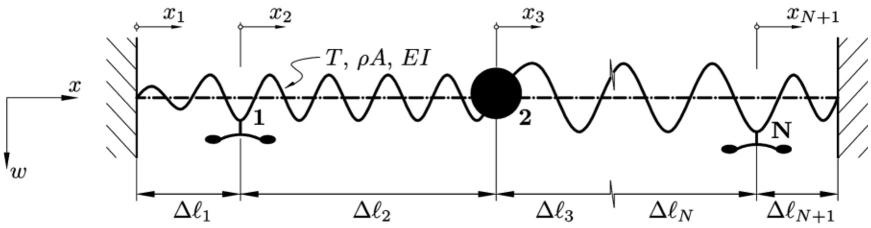

Fig. 1 Schematic view of a typical long span transmission line

$$EIw_n''''(x_n, t) + \rho A\ddot{w}_n(x_n, t) - Tw_n''(x_n, t) = f_w(x_n, t) + f_c(w_n, \dot{w}_n, t) \tag{1}$$

where EI is the bending stiffness of the conductor, T is the tension, ρA is the mass per unit length, $w_n(x_n, t)$ is the transverse displacement of the conductor at the location x_n and at time t, $f_w(x_n, t)$ is the wind force per unit length due to vortex shedding and $f_c(w_n, \dot{w}_n, t)$ represents the conductor's self damping. The primes stand for the partial differentiation with respect to the space coordinate x_n and the dots indicate the partial differentiation with respect to the time t. In the span, the points of attachment of the fittings are given by $x = l_1, l_2, l_3, ..., l_N$, and hence, the conductor can be divided into $(N+1)$ number of sub-spans with the span lengths $\Delta l_n = (l_n - l_{n-1})$; where $n = 1, 2, 3, ..., N+1$; with $l_0 = 0$ and $l_{N+1} = L$. Eq. (1) is valid for $0 \le x_n < \Delta l_n$, but $x_n \ne \Delta l_n$. At the point $x_n = \Delta l_n$ the fitting-clamp forces have to be taken into consideration.

The bending stiffness EI of the conductor in Eq. (1) is essential for the calculation of the bending stresses (in "bending boundary layers"), which are the primary reason for material fatigue. The bending stiffness is however small compared to the other parameters, i.e., $\sqrt{EI/T} \ll \lambda/2\pi$. Its influence on the eigenfrequencies and eigenfunctions of the free vibrations ($f_w(x_n, t) = f_c(w_n, \dot{w}_n, t) = 0$) can therefore be neglected (Claren and Diana 1966). The overall vibration levels are thus first estimated without paying any attention to the bending stiffness. The bending strains are determined afterwards, using the computed vibration amplitudes and singular perturbations. Neglecting the stiffness EI in Eq. (1) as well as omitting the right hand side, gives the wave equation

$$\rho A\ddot{w}_n(x_n, t) - Tw_n''(x_n, t) = 0 \qquad \text{for} \quad n = 1, 2, 3, ..., N+1 \tag{2}$$

The eigenvalue problem described by Eq. (2) combined with the boundary conditions at the span ends as well as at the location of the in-span fittings will give the complex eigenmodes needed for the EBP. Before formulating the boundary conditions it is convenient to re-scale the basic variables. This improves the numerical behavior of the eigenvalue problem which is otherwise very poorly conditioned. We first normalize the time t with respect to the fundamental frequency of the system and the space coordinates for each sub span x_n with respect to its length as

$$\tau = \left(\frac{\pi c}{L}\right)t, \qquad \eta_n = \frac{x_n}{\Delta l_n} \tag{3}$$

From Eq. (2) we obtain the equation of motion for the free vibrations in terms of the normalized coordinates for the nth sub-span as

$$\frac{\partial^2 \tilde{w}_n}{\partial \eta_n^2} - \left(\frac{\Delta l_n \pi}{L}\right)^2 \frac{\partial^2 \tilde{w}_n}{\partial \tau^2} = 0 \tag{4}$$

Here $\tilde{w}_n = w_n / D$ is the normalized displacement, c is the wave velocity given by $c = \sqrt{T/\rho A}$ and D is the diameter of conductor. Separation of variables in Eq. (4) and introducing the unknown complex parameters $\tilde{s}$ leads to

$$\tilde{w}_n(\eta_n, \tau) = \tilde{W}_n(\eta_n) e^{\tilde{s}\tau} \tag{5}$$

From Eq. (4) the solution for $\tilde{W}_n(\eta_n)$ can be written as

$$\tilde{W}_n(\eta_n) = \tilde{A}_n e^{(\Delta l_n \pi / L)\tilde{s}\eta_n} + \tilde{B}_n e^{-(\Delta l_n \pi / L)\tilde{s}\eta_n} \tag{6}$$

The parameter $\tilde{s} = s(L/\pi c)$ is actually the normalized eigenvalue of the system with respect to the fundamental frequency of the string; the imaginary part of s represents a frequency, the real part a decay coefficient. Assuming that the clamps at the ends of the span remain fixed gives the boundary conditions

$$w_1(0, t) = 0 \text{ and } w_{N+1}(\Delta l_{N+1}, t) = 0 \tag{7}$$

which, in normalized coordinates is written as

$$\tilde{w}_1(0, \tau) = 0 \quad \text{and} \quad \tilde{w}_{N+1}(1, \tau) = 0 \tag{8}$$

Substituting into the expressions for $\tilde{w}$ from Eq. (5) and Eq. (6) yields

$$\tilde{A}_1 + \tilde{B}_1 = 0 \tag{9}$$

and

$$\tilde{A}_{N+1} e^{(\Delta l_{N+1}\pi/L)\tilde{s}} + \tilde{B}_{N+1} e^{-(\Delta l_{N+1}\pi/L)\tilde{s}} = 0 \tag{10}$$

2.1. Compatibility conditions

2.1.1. For the Stockbridge damper

Now we formulate compatibility conditions at the points of attachment of the fittings. Fig. 2 shows the forces and the displacements at the damper clamp. For compatibility of the displacements $w(t)$ has to be continuous at $x_n = \Delta l_n$, that is

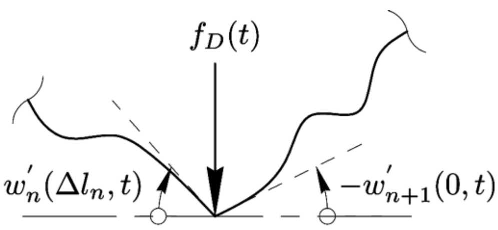

Fig. 2 Forces at the damper clamp

$$w_n(\Delta l_n, t) = w_{n+1}(0, t) \tag{11}$$

which, in terms of normalized variables can be written as

$$\tilde{w}_n(1, \tau) = \tilde{w}_{n+1}(0, \tau) \tag{12}$$

Substituting into the expressions for $\tilde{w}$ from Eq. (5) and Eq. (6) leads to

$$\tilde{A}_n e^{(\Delta l_n \pi / L)\tilde{s}} + \tilde{B}_n e^{-(\Delta l_n \pi / L)\tilde{s}} - \tilde{A}_{n+1} - \tilde{B}_{n+1} = 0 \tag{13}$$

At the point of attachment of a Stockbridge damper to the conductor (x_D), the damper clamp exerts a force (f_D) on the conductor, the complex amplitude of this force being given by

$$\widehat{f_D} = Z(s)\widehat{\dot{w}}(x_D) \tag{14}$$

where $\widehat{f_D}$ and $\widehat{\dot{w}}$ are the complex amplitudes respectively of the force and of the velocity at the damper clamp. The complex impedance $Z(s)$ of the Stockbridge damper is known from laboratory experiments, which is a function of velocity and the frequency of the vibration of the damper clamp. At this degree of modeling, the rotation of the damper clamp and its length are disregarded, although they can be taken into account in more detailed models. On the other hand, the damper force is given by (refer Fig. 2)

$$f_D(t) = T[w'_{n+1}(0, t) - w'_n(\Delta l_n, t)] \tag{15}$$

Expressing the damper force amplitude through the impedance, and using Eq. (5), Eq. (6) and Eq. (15)

$$\tilde{A}_n e^{(\Delta l_n \pi / L)\tilde{s}} - \tilde{B}_n e^{-(\Delta l_n \pi / L)\tilde{s}} + \tilde{A}_{n+1}[\tilde{Z}(\tilde{s}) - 1] + \tilde{B}_{n+1}[\tilde{Z}(\tilde{s}) + 1] = 0 \tag{16}$$

where the normalized impedance $\tilde{Z}(\tilde{s}) = \{Z(s)c/T\}$ was introduced.

2.1.2. For the aircraft warning sphere

In long span transmission lines, specially those near to the air fields, it often is required to attach aircraft warning spheres to the transmission lines to warn aircraft pilots. These spheres can either be hung to the line at single points or be attached as two halves, with the conductor passing through it. In the first case they can again be modeled by their impedance, which will simply be an imaginary quantity (same as impedance for a pure mass). In the following part of current section, we shall deal with the second case and assume that the spheres are attached via two clamps rigidly fixed at the spheres, modeled as rigid bodies.

Fig. 3 shows a rigid body representing a warning sphere attached to the conductor. The transverse force components acting on the body at points **1** and **2** satisfy the equation

$$\begin{Bmatrix} F_{1n} \\ F_{2n} \end{Bmatrix} = [\mathbf{M}] \begin{Bmatrix} \ddot{y}_1 \\ \ddot{y}_2 \end{Bmatrix} \tag{17}$$

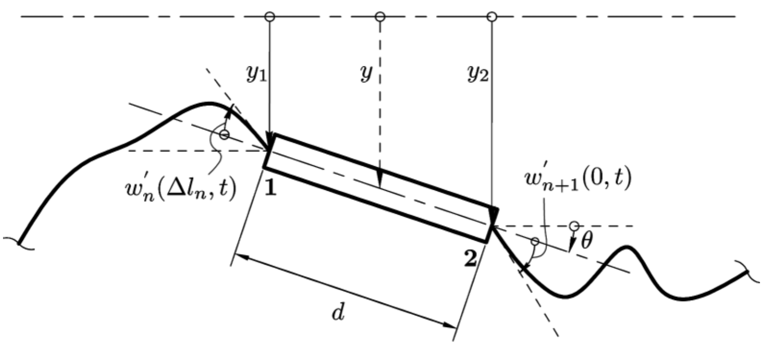

Fig. 3 Forces on the warning sphere as a rigid body

The mass matrix **M** for the warning sphere corresponding to the shown coordinate system is

$$\mathbf{M} = \begin{bmatrix} m_{11} & m_{12} \\ m_{21} & m_{22} \end{bmatrix} \tag{18}$$

where $m_{11} = m_{22} = \{(M/4)+(J/d^2)\}$ and $m_{12} = m_{21} = \{(M/4)-(J/d^2)\}$. M represents the mass of the warning sphere included with clamp-masses, J the mass moment of inertia of the sphere with clamps and d represents the diameter of the sphere.

Since the transverse force components are produced by the conductor tension, we have

$$F_{1n} = T(y_1' - \theta) \quad \text{and} \quad F_{2n} = T(\theta - y_2') \tag{19}$$

where $\theta = \{(y_2 - y_1)/d\}$, $y_1 = w_n(\Delta l_n, t)$ and $y_2 = w_{n+1}(0, t)$. Substituting into the expressions for w, F_{1n} and F_{2n} from Eq. (5), Eq. (6) and Eq. (17), we ultimately get the following equations

$$\begin{aligned} &\tilde{A}_n\left[\left(\frac{\pi c}{L}\right)^2\tilde{s}^2 m_{11} - \frac{T}{L}\pi\tilde{s} - \frac{T}{d}\right]e^{(\Delta l_n \pi/L)\tilde{s}} + \tilde{B}_n\left[\left(\frac{\pi c}{L}\right)^2\tilde{s}^2 m_{11} + \frac{T}{L}\pi\tilde{s} - \frac{T}{d}\right]e^{-(\Delta l_n \pi/L)\tilde{s}} \\ &\quad + \tilde{A}_{n+1}\left[\left(\frac{\pi c}{L}\right)^2\tilde{s}^2 m_{12} + \frac{T}{d}\right] + \tilde{B}_{n+1}\left[\left(\frac{\pi c}{L}\right)^2\tilde{s}^2 m_{12} + \frac{T}{d}\right] = 0 \end{aligned} \tag{20}$$

and

$$\begin{aligned} &\tilde{A}_n\left[\left(\frac{\pi c}{L}\right)^2\tilde{s}^2 m_{21} + \frac{T}{d}\right]e^{(\Delta l_n \pi/L)\tilde{s}} + \tilde{B}_n\left[\left(\frac{\pi c}{L}\right)^2\tilde{s}^2 m_{21} + \frac{T}{d}\right]e^{-(\Delta l_n \pi/L)\tilde{s}} \\ &\quad + \tilde{A}_{n+1}\left[\left(\frac{\pi c}{L}\right)^2\tilde{s}^2 m_{22} + \frac{T}{L}\pi\tilde{s} - \frac{T}{d}\right] + \tilde{B}_{n+1}\left[\left(\frac{\pi c}{L}\right)^2\tilde{s}^2 m_{22} - \frac{T}{L}\pi\tilde{s} - \frac{T}{d}\right] = 0 \end{aligned} \tag{21}$$

3. The eigenvalue problem and its solution

Eq. (9), Eq. (10), Eq. (13), Eq. (16), Eq. (20) and Eq. (21) together give a transcendental set of

$2(N+1)$ linear homogeneous equations, which can be written as

$$\mathbf{J}(\tilde{s})\mathbf{a} = \mathbf{0} \tag{22}$$

In this equation one has

$$\mathbf{J}(\tilde{s}) = \begin{bmatrix} 1 & 1 & 0 & 0 & 0 & \cdot\cdot & 0 & 0 & 0 & 0 \\ P^-_{1,1}\Lambda^+_1 & P^+_{1,1}\Lambda^-_1 & -P^-_{2,1} & -P^-_{2,1} & 0 & \cdot\cdot & 0 & 0 & 0 & 0 \\ P^+_{2,1}\Lambda^+_1 & -P^-_{2,1}\Lambda^-_1 & P^+_{3,1} & P^-_{3,1} & 0 & \cdot\cdot & 0 & 0 & 0 & 0 \\ 0 & 0 & P^-_{1,2}\Lambda^+_2 & P^+_{1,2}\Lambda^-_2 & * & \cdot\cdot & 0 & 0 & 0 & 0 \\ 0 & 0 & P^+_{2,2}\Lambda^+_{2,2} & -P^-_{2,2}\Lambda^-_{2,2} & * & \cdot\cdot & 0 & 0 & 0 & 0 \\ \cdots & \cdots & \cdots & \cdots & \cdots & \cdot\cdot & \cdots & \cdots & \cdots & \cdots \\ \cdots & \cdots & \cdots & \cdots & \cdots & \cdot\cdot & \cdots & \cdots & \cdots & \cdots \\ 0 & 0 & 0 & 0 & 0 & \cdot\cdot & P^-_{1,N+1}\Lambda^+_{N+1} & P^+_{1,N+1}\Lambda^-_{N+1} & -P^-_{2,N+1} & -P^-_{2,N+1} \\ 0 & 0 & 0 & 0 & 0 & \cdot\cdot & P^+_{2,N+1}\Lambda^+_{N+1} & -P^-_{2,N+1}\Lambda^-_{N+1} & P^+_{3,N+1} & P^-_{3,N+1} \\ 0 & 0 & 0 & 0 & 0 & \cdot\cdot & 0 & 0 & \Lambda^+_{N+1} & \Lambda^-_{N+1} \end{bmatrix} \tag{23}$$

and

$$\mathbf{a} = \langle \tilde{A}_1, \tilde{B}_1, \tilde{A}_2, \tilde{B}_2, ..., ..., \tilde{A}_{N+1}, \tilde{B}_{N+1} \rangle^T \tag{24}$$

where

$$\Lambda^+_n = e^{(\Delta l_n \pi/L)\tilde{s}}, \quad \Lambda^-_n = e^{-(\Delta l_n \pi/L)\tilde{s}}; \quad \text{for} \quad n = 1, 2, 3, ..., N+1$$

Table 1 Variable P for different line fittings

Variables	For Stockbridge damper	For warning sphere
$P^+_{1,n}$	1	$\left(\frac{\pi c}{L}\right)^2 \tilde{s}^2 m_{11} + \frac{T}{L}\pi\tilde{s} - \frac{T}{d}$
$P^-_{1,n}$	1	$\left(\frac{\pi c}{L}\right)^2 \tilde{s}^2 m_{11} - \frac{T}{L}\pi\tilde{s} - \frac{T}{d}$
$P^+_{2,n}$	1	$\left(\frac{\pi c}{L}\right)^2 \tilde{s}^2 m_{12} + \frac{T}{d}$
$P^-_{2,n}$	1	$-\left\{\left(\frac{\pi c}{L}\right)^2 \tilde{s}^2 m_{12} + \frac{T}{d}\right\}$
$P^+_{3,n}$	$\tilde{Z} - 1$	$\left(\frac{\pi c}{L}\right)^2 \tilde{s}^2 m_{22} + \frac{T}{L}\pi\tilde{s} - \frac{T}{d}$
$P^-_{3,n}$	$\tilde{Z} + 1$	$\left(\frac{\pi c}{L}\right)^2 \tilde{s}^2 m_{22} - \frac{T}{L}\pi\tilde{s} - \frac{T}{d}$

The values of the variables $P_{1,n}^{+}, P_{1,n}^{-}, P_{2,n}^{+}, P_{2,n}^{-}, P_{3,n}^{+}$ and $P_{3,n}^{-}$ in Eq. (23) depend on whether the corresponding fitting is a Stockbridge damper or a warning sphere. In Table 1, values of these variables are given.

Since the matrix $\mathbf{J}(\tilde{s})$ contains the system parameters we will refer to it as the system matrix. It can be seen that the elements of the system matrix are transcendental functions of the parameter $\tilde{s}$. The matrix equation constitutes an eigenvalue problem having infinitely many eigenvalues. Note that the eigenvalues of the original system are the values of the parameter $\tilde{s}$ multiplied with the fundamental frequency of the string (i.e. $(\pi c/L)$).

3.1. Solution of the eigenvalue problem

One technique of solving the transcendental eigenvalue problem is by the determinant search method, where one searches for values of $\tilde{s}$ for which $\det(\mathbf{J}(\tilde{s}))$ becomes zero (Hagedorn, *et al*. 2002). This is only possible for relatively small system matrices. Due to the poor numerical behavior of the system matrix $\mathbf{J}(\tilde{s})$, it is easy to miss many values of $\tilde{s}$ for which actually the determinant of $\mathbf{J}(\tilde{s})$ is zero. Though normalization of the basic variables leads to a better conditioned system matrix, however, difficulties were faced by the authors when trying to find the eigenvalues of very big system with the determinant search method. The prime reasons for these difficulties are large differences in the order of numerical values of the elements of system matrix, which, together with the large number of algebraic operations involved in calculating the determinant lead to numerical problems. Moreover, the two dimensional search domain (i.e. complex domain) adds up the difficulties.

To overcome these difficulties an alternate approach was used by the authors, in which the homogeneous set of $2N+2$ simultaneous equations, given by Eq. (22), is first transformed into a non-homogeneous system by using the first $2N+1$ equations. A simple and better conditioned optimization criterion is then defined for the last equation. The steps are described in more details in the following lines:

1. Let $A_1 = 1$.
2. Substitute the value of A_1 into the first $2N+1$ homogeneous equations of Eq. (22) will transform them into a set of non-homogeneous equations. Determine $B_1, A_2, B_2, A_3, B_3, \ldots, A_{N+1}, B_{N+1}$ by solving these $2N+1$ equations.
3. Substitute the values of $B_1, A_2, B_2, A_3, B_3, \ldots, A_{N+1}, B_{N+1}$ into $2N+2^{nd}$ equation. Since these are not the correct values, these will not satisfy this equation and will result in an error ε as given by

$$\begin{aligned} &J_{(2N+2),1}(\tilde{s})+B_1 J_{(2N+2),2}(\tilde{s})+A_2 J_{(2N+2),3}(\tilde{s})+B_2 J_{(2N+2),4}(\tilde{s})+\ldots \\ &\qquad +A_{N+1} J_{(2N+2),(2N+1)}(\tilde{s})+B_{N+1} J_{(2N+2),(2N+2)}(\tilde{s})=\varepsilon \end{aligned} \tag{25}$$

4. Minimize the error ε with respect to the eigenvalue $\tilde{s}$.

This procedure resulted in a rapidly converging method. Hence, one can always be sure that the value of $\tilde{s}$ one is finding after minimizing ε, is an eigenvalue of the system in Eq. (22). In the present work this approach has been adopted, which ultimately resulted in finding most if not all of the first thousand or so eigenvalues $\tilde{s}$ of the normalized system. The entire coding was done in MATLAB 6.5, and for minimizing the ε, among others the in-built function “fsolve” was used.

After finding the eigenvalues $\tilde{s}$ of the system matrix, the corresponding eigenvectors were found by solving an equivalent algebraic matrix eigenvalue problem of the form

$$[\mathbf{J}(\tilde{s}) - \lambda I]\mathbf{a} = \mathbf{0} \tag{26}$$

The eigenvector corresponding to any eigenvalue $\tilde{s}$ of the transcendental eigenvalue problem (22) is obtained by finding the eigenvector associated to $\lambda = 0$ in the equivalent algebraic eigenvalue problem of Eq. (26), where $\tilde{s}$ has been determined beforehand.

4. Application of the energy balance principle

In Eq. (1) the parameters on the right hand side are not known in detail. Due to this fact in the EBP the problem is simplified further. First, the wind speed is assumed to change slowly with respect to the conductor's oscillations in the frequency range of 3 to 50 Hz, so that stationary oscillations can be assumed. For a given constant speed of transverse wind a lift force then acts on the conductor in first approximation as a harmonic time function of frequency f_s proportional to the wind speed, as given by the Strouhal's relation,

$$f_s = S\frac{U}{D} \tag{27}$$

where U is the wind speed, D the conductor diameter and S (≈ 0.2) is the Strouhal's number, and the conductor is assumed to oscillate with frequency f_s (lock-in frequency).

Using this simplified model (Bahtovska 2000, Hadulla 2000) and assuming that the shape of the conductor vibration is given by the eigenfunction associated to the corresponding resonance frequency, the conductor vibration amplitudes can be approximately computed as a function of the wind speed perpendicular to the conductor using energy balance in the form

$$P_W = P_D + P_C \tag{28}$$

In Eq. (28) P_W is the power input of the aerodynamic forces in steady state, P_D is the mechanical energy dissipated by the conductor fittings and P_C is the power dissipated by the structural damping in the conductor. While of course all these powers are functions of time, the expressions in Eq. (28) are the time averages. Each of these terms is then a function of both, the frequency and of the amplitude of the conductor oscillations. For a given wind speed, or frequency, Eq. (28) is a nonlinear algebraic equation in the amplitude of conductor oscillations only.

4.1. Power dissipated by the fittings

The power dissipated in the Stockbridge damper is a function of the motion of the damper clamp. For a linear damper model it is related to its complex impedance. But also in the case of a "nonlinear damper" the experimental determination of the dependence of P_D on the clamp motion in first approximation poses no problem, at least as long as the the clamp motion is harmonic. The measurement of the complex impedance of a Stockbridge damper is routinely done in vibration laboratories. The impedance Z_ν ($\nu = 1, 2, 3, \ldots, N$) of the νth damper, the power dissipated in the damper is given by Hadulla (2000)

$$P_{D,\nu} = \frac{\omega^2}{2}\mathbb{R}[\hat{q}^*_{cl,\nu} Z^*_\nu \hat{q}_{cl,\nu}] \tag{29}$$

Since warning sphere is modeled as a pure mass, impedance value for it is a completely imaginary quantity, and hence, it dissipates no power. The sum of the terms in Eq. (29) for all the Stockbridge dampers gives the total power dissipated by the conductor fittings P_D. It will of course be a function of the frequency and local vibration amplitudes, which, up to a scaling factor, are given by the corresponding complex eigenmode.

4.2. Wind power input

The situation is quite different for the wind power input P_W. It is not very difficult to measure the transversally pulsating force acting on a fixed rigid cylinder immersed in a wind tunnel under stationary laminar flow, and these experiments have been carried out by several authors, e.g., Bishop and Hassan (1964). The situation is more complicated for a vibrating rigid cylinder, e.g., Diana and Falco (1971), Staubli (1979), Chen (1987) or a flexible cylinder, e.g., Rawlins (1983), Brika and Laneville 1995) in harmonic transversal motion, where the forces not only depend on the vibration amplitudes but also on the ratio between the oscillation frequency and the Strouhal frequency. The power becomes particularly large if the two frequencies are approximately equal. Moreover, for a forced harmonic motion of the cylinder with a frequency in the neighborhood of f_s, the vortices will be generated with the driving frequency instead of the Strouhal frequency (viz. lock-in phenomenon). The force remains no longer harmonic, particularly for very small vibration amplitudes, where both the frequencies, the driving frequency and the Strouhal frequency, are present on the oscillating forces. The dependence of the force on the amplitude A is very important for the large amplitudes. It is not surprising that for very large amplitudes the power P_W becomes even negative, the cylinder then imparts energy back to the fluid. For the reasonably large vibration amplitudes the aerodynamic forces can be assumed to be harmonic with the same frequency as the oscillation, the wind power input being given by

$$P_W(f, A) = Lf^3 D^4 \mathbb{F}\left(\frac{A}{D}\right) \tag{30}$$

the function $\mathbb{F}(A/D)$ being obtained experimentally. Experimental data on the wind power input are given and compared with each other for example in Belloli, *et al.* (2003). Often such functions are approximated by polynomials and for the present computations the following expression for $\mathbb{F}(A/D)$ has been used

$$\begin{aligned}\mathbb{F}\left(\frac{A}{D}\right) = {} & 2.2727\left(\frac{A}{D}\right) + 88.006\left(\frac{A}{D}\right)^2 - 180.8919\left(\frac{A}{D}\right)^3 \\ & + 480.0356\left(\frac{A}{D}\right)^4 - 1810.7\left(\frac{A}{D}\right)^5 + 2844.0\left(\frac{A}{D}\right)^6 - 1557.2\left(\frac{A}{D}\right)^7\end{aligned} \tag{31}$$

This particular polynomial corresponds to the data published in Rawlins (1983). In Eq. (30) and Eq. (31) the variable A is the local vibration amplitude of the conductor undergoing harmonic oscillation. For a conductor vibrating in a shape corresponding to a [complex] eigenfunction, the wind power is obtained by integration over the span, as explained for the case of bundled conductors in Hagedorn, *et al.* (2002). The wind power input of course depends on the degree of turbulence of the wind flow, but only few attempts have so far been made to measure the vibration levels and wind data in the actual conductor of transmission lines under real working conditions.

4.3. Structural damping

The power dissipated by structural damping in the conductor is sometimes measured by conductor manufacturers and also in other vibration laboratories. It is a function not only of the amplitude and of the frequency but also of the tension in the conductor. For higher tension the structural damping usually decreases. P_C has been investigated by several authors like Noiseux (1992). Different laboratories use distinct empirical formulas obtained from experiments with particular conductors. For the present computations the following empirical expression, obtained by the personal communication from RIBE Elektroarmaturen GmbH & Co. KG Schwabach, has been used

$$P_C = 2160 f^{N_f} \left(\frac{180}{\pi} B \right)^{N_b} \left(\frac{P}{T^{N_t}} \right) LC \tag{32}$$

where C, N_f, N_b and N_t are constants. It is usually assumed that N_f, N_b and N_t are constant for all conductors and that C characterizes the damping properties of the particular conductor being considered. The variable B is the vibration angle in radians $\{= (\pi/180)\beta = (\pi/180)(\omega/c)A\}$ and P is the rated tensile strength of the conductor. As defined in Eq. (30) and Eq. (31), A is the local vibration amplitude of the conductor and ω is the circular frequency corresponding to the eigenvalue under consideration.

The numerical solution of Eq. (28) is a relatively simple task and the results shown in Section 6 (Figs. 5, 6, 7, 8, 9, 10, 11 and 12), are obtained in this manner. For a conductor without a Stockbridge damper, the term P_D vanishes and the amplitude is then simply obtained from $P_W = P_C$. If however dampers are attached, they dissipate much more power than does the conductor's self damping, i.e., $P_D \gg P_C$. In such a case, the amplitudes can simply be obtained by $P_W = P_D$. Once the vibration amplitudes are known as a function of the frequency or wind speed, bending strains can be computed via singular perturbation as shown in Hagedorn (1980) and Cole (1968).

5. Example problem

This example problem shows, how the appropriate placement of the dampers can be helpful in

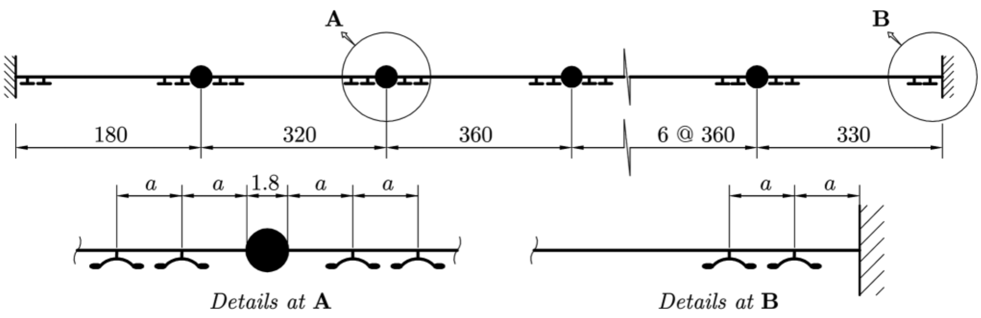

Case-1	$a = 3.5\ m$
Case-2	$a = 1.0\ m$

Fig. 4 Example problem (all dimensions in meter)

increasing the life of transmission line by keeping its critical strains and amplitudes within the safe limits. As shown in Fig. 4, a very long transmission line span of 3350 m has been considered, carrying nine warning spheres, which are attached respectively at 180 m, 500 m, 860 m, 1220 m, 1580 m, 1940 m, 2300 m, 2660 m and 3020 m from the left end. Groups of two Stockbridge dampers are attached at both the span-ends, and in proximity of the warning spheres. The diameter of the conductor is 33.95 mm, its mass per unit length is 2.95 kg/m and the conductor tension is 121.7 kN. All warning spheres and Stockbridge dampers are taken of the same type. The diameter of one warning sphere is 1.8 m, its mass is 45.6 kg and its mass moment of inertia is 17.5 kg m^2.

From the span length L, conductor tension T and its unit mass ρA the wave velocity (i.e. $c = \sqrt{T/\rho A}$), fundamental frequency of conductor without any fitting on it (i.e. $\omega_0 = \pi c/L$) and the minimum possible wavelength (i.e. $\lambda_{\min} = c/f_{\max}$) can be calculated; where $f_{\max}$ is the maximum frequency under consideration in Hz. For efficient damping two consequent dampers in a damper-group should always be placed so that both of them must never fall on the nodes at the same time, for any vibration frequency of the conductor under the considered frequency range. For fulfilling this criterion it is taken as a thumb-rule by the practice engineers, to provide two consequent dampers in a damper-group with an approximate maximum spacing of $0.22\lambda_{\min}$ to $0.25\lambda_{\min}$. The same is true for the spacing of the last dampers from the span-ends, so that they do not fall on the nodes for any of the vibration frequencies of conductor.

The problem has been solved for two different damper spacings to show its influence on the maximum strains and the maximum span amplitudes. In the first case the damper spacing has been kept as 3.5 m and in the second case same has been taken as 1 m. The eigenvalue problem was solved in the frequency domain of 3 to 50 Hz and the damping ratios of the different eigenvalues are plotted in Fig. 5 for the first case and in Fig. 9 for the second case. These figures show the effective damping corresponding to the natural frequencies of the system. Fig. 6 and Fig. 10 show

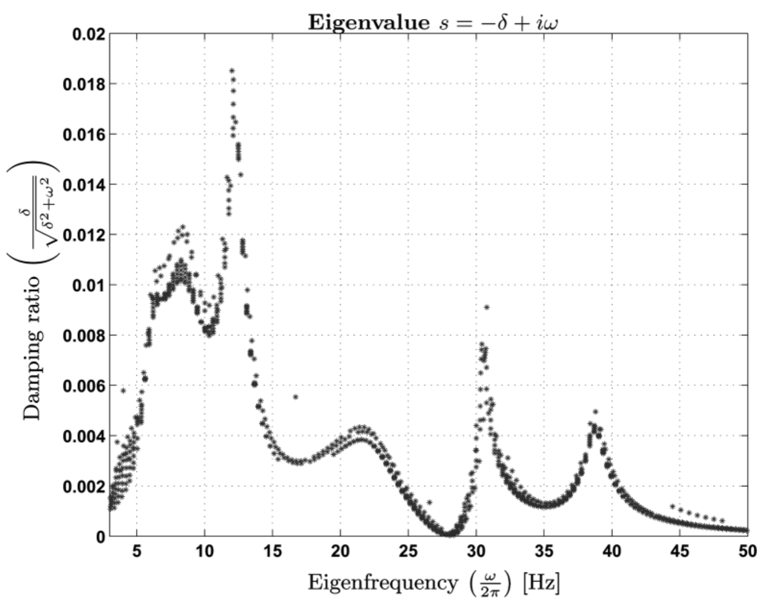

Fig. 5 Eigenvalues of the system (Case-1)

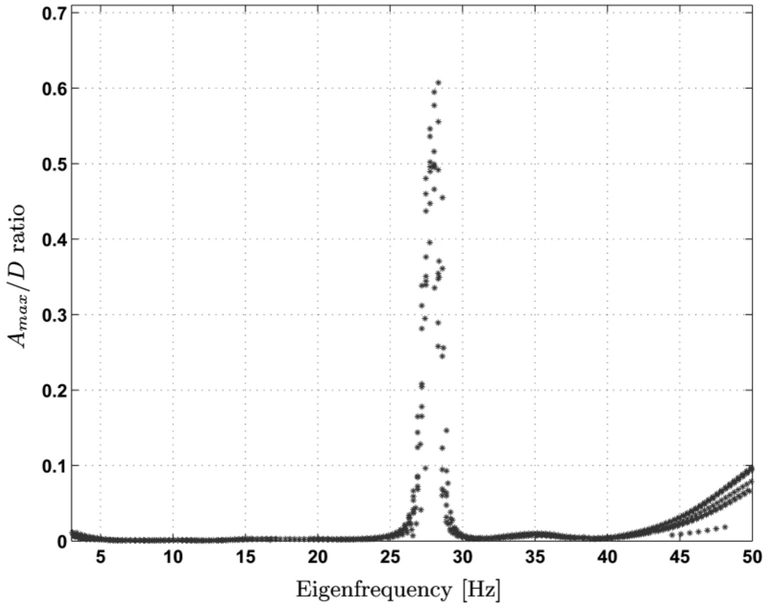

Fig. 6 $A_{\max}/D$ ratio (Case-1)

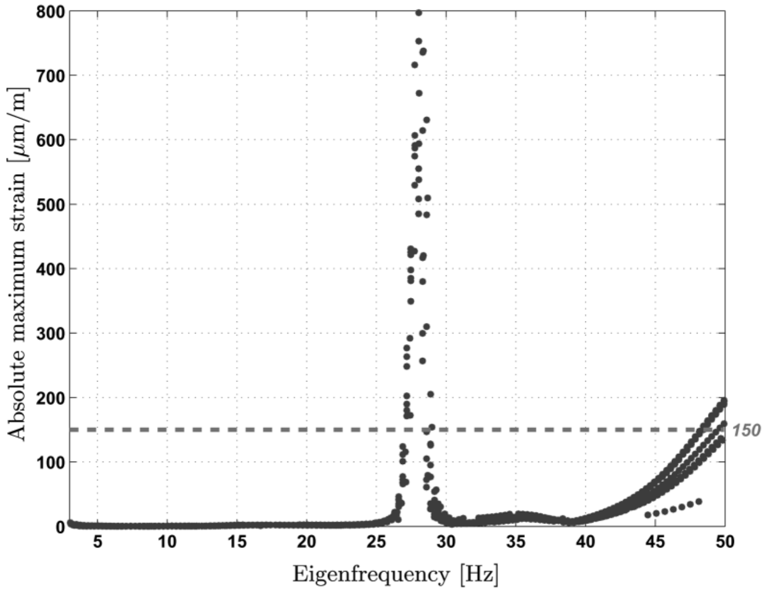

Fig. 7 Absolute maximum strains (Case-1)

the results of EBP: the maxima of the local vibration amplitudes (maxima with respect to the span) are shown as a function of the frequency. Note that for each frequency these maxima will occur at different locations of the conductor. After obtaining the actual amplitude, the strains at critical points, i.e., clamped-ends and the damper-clamps, are calculated taking into account the bending

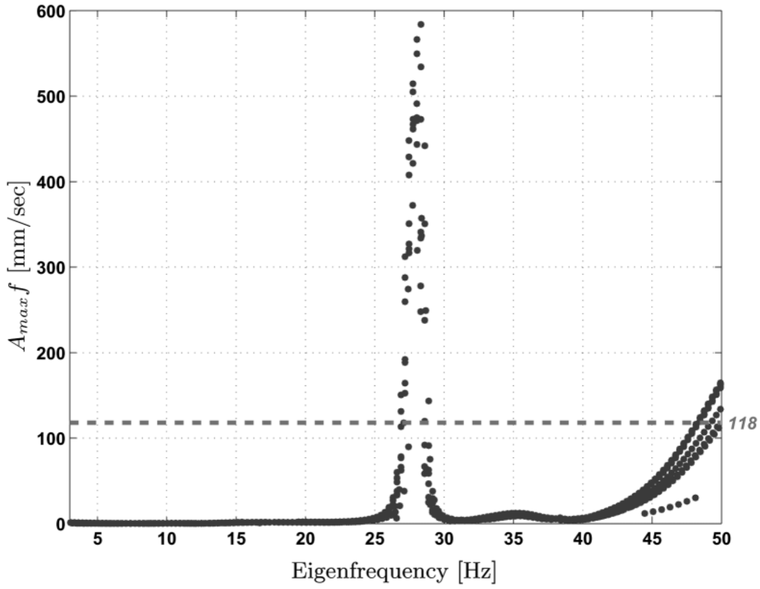

Fig. 8 Product of maximum span amplitudes by vibration frequency (Case-1)

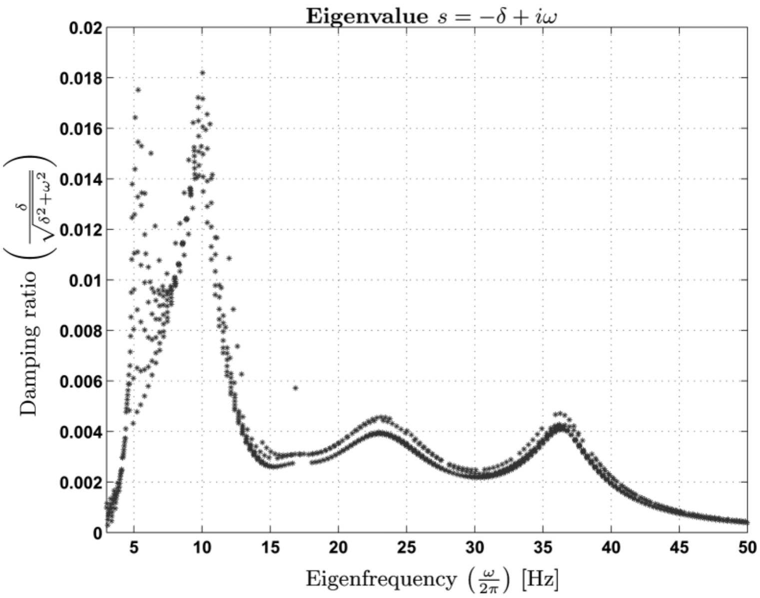

Fig. 9 Eigenvalues of the system (Case-2)

stiffness of the conductor. Fig. 7, Fig. 11 and Fig. 8, Fig. 12 correspondingly show the maximum strains and the values of $A_{\max} \cdot f$ in the span for different natural frequencies, for both the cases respectively.

In the case of present problem the maximum frequency under consideration is 50 Hz. The wave velocity in the conductor is 203.13 m/sec and hence the possible minimum wavelength is 4.06 m

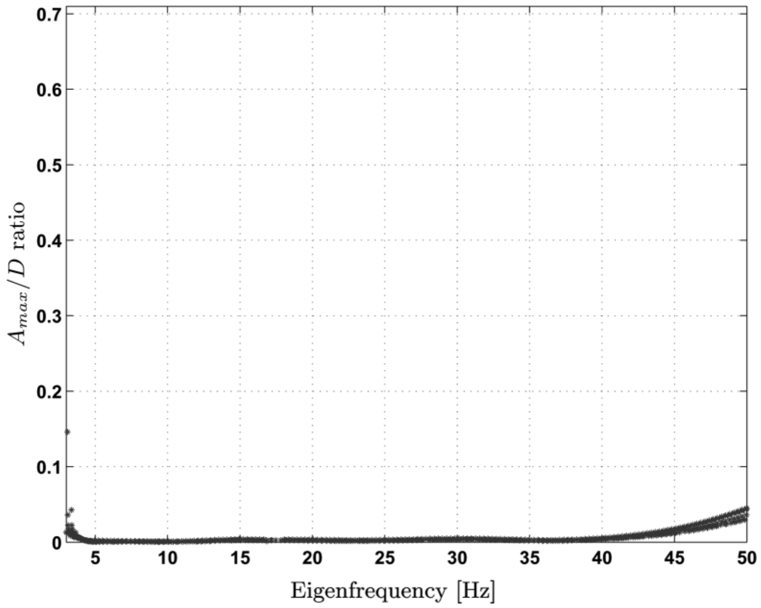

Fig. 10 $A_{\max}/D$ ratio (Case-2)

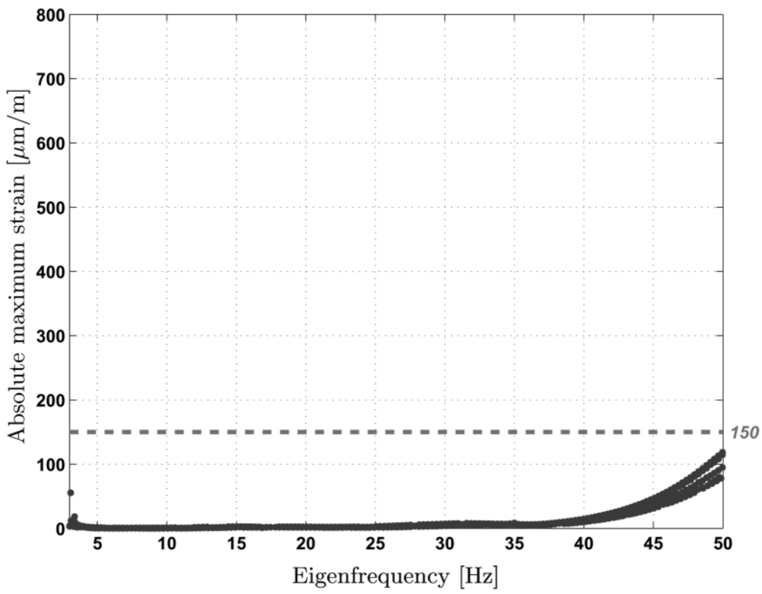

Fig. 11 Absolute maximum strains (Case-2)

(i.e. $\lambda_{\min} \approx 4$ m). This means that for the efficient damping two consequent dampers in a damper-group should be kept at a maximum distance of approximately 1 m, which will make it sure that both the dampers will never fall on nodes simultaneously, for any natural frequency of the system under 50 Hz. In the first case when the dampers are at 3.5 m apart in each group, this fact can be

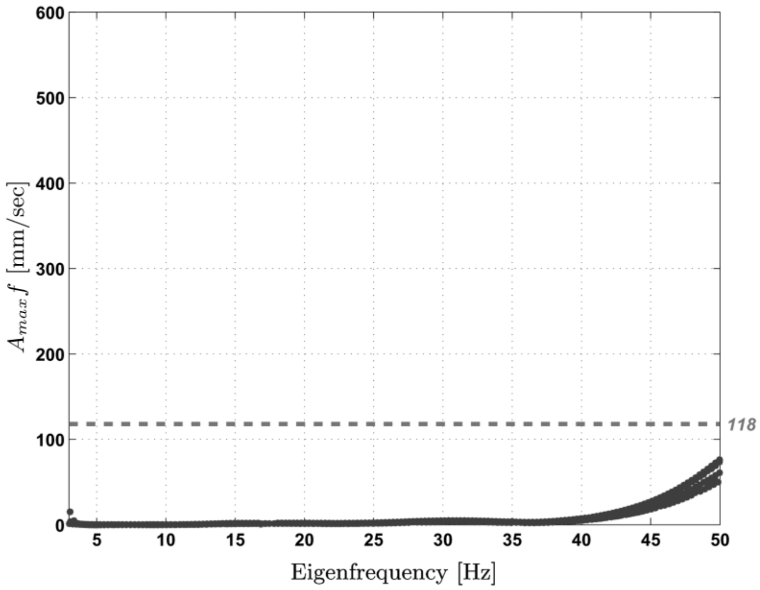

Fig. 12 Product of maximum span amplitudes by vibration frequency (Case-2)

easily verified from Fig. 7 and Fig. 8 that, when the dampers are kept at the spacings in the range of the possible minimum wavelength, maximum strains and amplitudes cross the permitted limiting values (i.e. 150 μm/m for the maximum strain and 118 mm/sec for the $A_{\max} f$ value). The 0.5λ value corresponding to the frequencies 25−30 Hz fall in the range of 4.06−3.39 m respectively. The provided damper spacing for the first case falls in this range (i.e. 3.5 m). It can therefore be seen in Fig. 7 and Fig. 8 that one gets peaks in the strain and the span amplitude curves in 25−30 Hz range, because for this frequency range both the dampers in each group will fall on the node simultaneously. Hence, they will not be able to damp out the vibrations of the frequencies 20−30 Hz. Whereas, with the same number of dampers when the placement of dampers is decided intelligently, and they are kept in the range of $0.22\lambda_{\min}$ to $0.25\lambda_{\min}$ (i.e. ≈ 1 m), it keeps the maximum strains and the amplitudes within the permissible limits (Fig. 11 and Fig. 12). Because, if one damper in the group now falls on the node, one can be sure that the second damper will never be on the node, and hence, out of two dampers at least one will always work.

6. Conclusions

In this paper the energy balance principle was modified for a long span transmission line equipped with Stockbridge dampers and aircraft warning spheres. The complex eigenvalue problem is formulated and conditioned by normalizing the basic variables. It is then solved numerically with a new approach by transforming the homogeneous set of transcendental simultaneous equations into a non-homogeneous one, which results in a better conditioned optimization criterion than that in the general determinant search method. The complex eigen-functions are taken into account in the EBP. In addition of Stockbridge dampers, a simple model for aircraft warning spheres is also introduced, taking into account their masses and moments of inertia. This approach is used to calculate the vibration amplitudes via EBP and subsequently the bending strains are calculated by the formulae obtained from singular perturbation. Since the impedances and the location of the dampers as well as warning spheres are taken into account, the approach is a useful tool for the optimization of the dampers and their locations. One practical example problem for a long span transmission line was solved and results were discussed.

Acknowledgements

The authors acknowledge the support given by RIBE Elektroarmaturen GmbH & Co. KG Schwabach, Ministry of Hessen and DFG (German Research Foundation).

References

Allnut, J.G. and Rowbottom, M.D. (1974), “Damping of aeolian vibration on overhead lines by vibration dampers”, *Proceeding of Institute of Electrical and Electronic Engineers*, **121**, 1175-1178.

Bahtovska, E. (2000), “The energy balance for damped wind-excited vibrations”, *Facta Universitatis*, **1**(7), 769-773.

Belloli, M., Cigada, A., Diana, G. and Rocchi, D. (2003), “Wind tunnel investigation on vortex induced vibration of a long flexible cylinder”, *Proceedings of Fifth International Symposium on Cable Dynamics, Santa Margherita*, Italy, 247-254, September.

Bishop, R.E.D. and Hassan, A.Y. (1964), “The Lift and Drag Forces on a Circular Cylinder in a Flowing Fluid”, In *Proceedings of the Royal Society of London 277* (Series A), 51-75.

Brika, D. and Laneville, A. (1995), “A laboratory investigation of the aeolian power imparted to a conductor using a flexible circular cylinder”, *Proceedings of the Royal Society of London 277(Series A)*, 23-27, July.

Chen, S.S. (1987), *Flow-Induced Vibration of Circular Cylindrical Structures*, Washington, New York, London: Hemisphere Publishing Corporation.

Claren, R. and Diana, G. (1966), “Vibrazioni dei conduttori”, *L’Energia Elettrica*, 10.

Cole, J. (1968), *Perturbation Methods in Applied Mathematics*, Waltham, Mass.

Dhotarad, M.S., Ganesan, N. and Rao, B.V.A. (1978), “Transmission line vibration”, *J. Sound Vib.*, **60**, 217-327.

Diana, G. and Falco, M. (1971), “On the forces transmitted to a vibrating cylinder by a blowing fluid”, *Mechanica*, **6**, 9-22.

EPRI (1979), *Transmission Line Reference Book, Wind Induced Conductor Motion*, Palo Alto, California: Electrical Power Research Institute.

Hadulla, T. (2000), *Wirbelerregte Schwingungen in Freileitungsbündeln*, PhD thesis, Institut für Mechanik, Technische Universität Darmstadt, Germany.

Hagedorn, P. (1980), “Ein einfaches Rechenmodell zur Berechnung winderregter Schwingungen an Hochspannungsleitungen mit Dämpfern”, *Ingenieur-Archiv*, **49**, 161-177.

Hagedorn, P. (1982), “On the computation of damped wind excited vibrations of overhead transmission lines”, *J. Sound Vib.*, **83**(2), 253-271.

Hagedorn, P., Mitra, N. and Hadulla, T. (2002), “Vortex-excited vibrations in bundled conductors: A mathematical model”, *J. Fluids Struct.*, **16**(7), 843-854.

Noiseux, D.U. (1992), “Similarity laws of the internal damping of stranded cables in transverse vibrations”, *IEEE Transections on Power Delivery*, **7**(3), 1574-1581, July.

Rawlins, C.B. (1983), “Wind tunnel measurements of the power imparted to a model of a vibrating conductor”, *IEEE Transactions on Power Apparatus & Systems*, **PAS-102**(4), 963-971, April.

Schäfer, B. (1981), *Zur Entstehung und Unterdrückung winderregter Schwingungen an Freileitungen*, PhD thesis, Technische Hochschule Darmstadt, Fachbereich Mechanik.

Staubli, T. (1979), “An investigation of the fluctuating forces on a transverse-oscillating circular cylinder”, In *EUROMECH-Colloquium 119*, London.

Verma, H., Chakraborty, G., Krispin, H.J. and Hagedorn, P. (2003), “On the modeling of wind induced vibrations of long span electrical transmission lines", *Proceedings of Fifth International Symposium on Cable Dynamics, Santa Margherita*, Italy, 53-60, September.

GS